A Theoretical Determination of the Efficiency with which Aerosol Particles are Collected by Simple Ice Crystal Plates

J. J. MARTIN, P. K. WANG AND H. R. PRUPPACHER

Department of Atmospheric Sciences, University of California, Los Angeles 90024

(Manuscript received 28 November 1979, in final form 24 March 1980)

ABSTRACT

Two theoretical models are presented which allow computing the efficiency with which aerosol particles of radius $0.001 \leq r \leq 10$ μm are collected by simple ice crystal plates of radius $50 \leq a_c \leq 640$ μm, in air of various relative humidity, temperature and pressure. Particle capture due to Brownian diffusion, thermophoresis, diffusiophoresis and inertial impaction is considered. It is shown that, analogous to water drops, ice crystal plates exhibit a minimum collection efficiency within a specific size interval of aerosol particles. This minimum is strongly affected by the relative humidity of the ambient air. The collection efficiency of particles with $r > 1$ μm is controlled by the flow field around the ice crystal, while the collection efficiency of particles with $r < 0.01$ μm is controlled by convective Brownian diffusion. Trajectory analysis predicts that aerosol particles are preferentially captured by the ice crystal rim. Our theoretical results are found to agree satisfactorily with laboratory studies presently available.

1. Introduction

Recent studies show that a substantial fraction of atmospheric aerosol particles is removed from the atmosphere and returned to the earth's surface by means of clouds and precipitation. Recent theoretical and experimental work on the efficiency with which aerosol particles are collected by cloud drops and rain drops has been summarized and critically reviewed by Wang *et al.* (1978), Grover *et al.* (1977), Slinn (1980) and Wang and Pruppacher (1977). Recent field studies on the scavenging of aerosol particles by rain have been discussed by Radke *et al.* (1978).

In contrast to the studies on scavenging of aerosol particles by water drops, little attention has been given to the scavenging of aerosol particles by ice crystals. However, the few field studies which exist on this subject point clearly to the fact that snow crystals play an important role in the removal of aerosol particles from the atmosphere. Thus, Reiter (1964), Reiter and Carnuth (1969) and Carnuth (1967) carried out field studies on the scavenging of aerosol particles by snow in storms over the German Alps. Graedel and Franey (1975) carried out similar field studies in the United States. Both of these field investigations showed that snow scavenges aerosol particles up to 50 times more efficiently than rain, when based on equal equivalent water content of the precipitation. A similar conclusion was reached by Itagaki and Koenuma (1962) and Magono *et al.* (1974, 1975) who made field studies in Japan and found that snow crystals of diameters between 400 and 1800 μm had collection efficiencies as large as 0.3–0.6.

Unfortunately, all the mentioned field studies are plagued by serious shortcomings which stem from the fact that they are based on observed changes in the aerosol particle concentration during a precipitation event. Such particle concentration changes may be the result of scavenging as well as the result of air mass changes which often accompany a precipitation event. In addition, the collision efficiencies derived from field studies usually apply to a wide spectrum of ice crystals and aerosol particle sizes, both changing in time. This makes it very difficult to extract from the observed data collection efficiencies which apply to an ice crystal of particle size collecting an aerosol particle of particular size. Also, the relative humidity, and thus the phoretic forces, usually vary greatly during the precipitation event.

Laboratory studies also point to the fact that ice crystals are efficient aerosol scavengers. Experiments involving natural snow crystals, generally of platelike type, were carried out by Knutson *et al.* (1976) and Sood and Jackson[1] in an outdoor chamber in the Chicago area. The aerosol particles studied had diameters between 0.5 and 7 μm and consisted of NaCl, latex, *B. Subtilis* spores, and a fluorescent material. The relative humidity in the aerosol pick-up

[1] Sood, S. K., and Jackson, M. R., 1970: Scavenging by snow and ice crystals. *Precipitation Scavenging—1970*, 121–136 [NTIS CONF-700601].

0022-4928/80/071628-11$06.75
© 1980 American Meteorological Society

chamber was typically between 0 and −10°C. The ice crystal studied had diameters > 1 mm. No attempt was made to study ice crystals with diameters < 1 mm and aerosol particles with diameters < 0.5 μm. Also, no attempt was made to study the effect of temperature and relative humidity of the air on the scavenging efficiency of the crystals. The only other experimental study known to the present authors on the scavenging efficiency of ice crystals is that of Starr and Mason (1966). Unfortunately, in their experiments only simulated ice crystals made from tissue paper were used. Therefore, the experiment of Starr and Mason took into account the effects of inertial impaction and Brownian motion but did not consider the effects of phoretic forces. Also, in the studies of Starr and Mason only ice crystal models of radius > 1 mm were considered.

Attempts to study the problem of aerosol particle scavenging on a theoretical basis have so far met with great difficulties. This is because theoretical descriptions of the flow field past ice crystals falling in the atmosphere have only recently become available. Thus, at present no theory is available that would quantitatively describe the efficiency with which aerosol particles are captured by ice crystals in ice-subsaturated or ice-supersaturated air. Such a theory would be highly desirable, considering that field studies have inherent inaccuracies and that laboratory experiments are usually confined to a very limited temperature, humidity and pressure range, while scavenging of aerosol particles in the atmosphere by ice crystals proceeds at all levels in the troposphere.

2. Present models

Motivated by the abovementioned deficiencies in our knowledge on the scavenging of aerosol particles by ice crystals we embarked on a series of theoretical studies in which we applied the methods of Grover *et al.* (1977) and Wang *et al.* (1978) to simple ice crystal plates.

Following the work of Grover *et al.* (1977), Pitter (1977) and Martin *et al.* (1980) a model was formulated (henceforth called model I) to compute the efficiency with which aerosol particles of radius $r > 0.1$ μm are collected by simple ice crystal plates. This efficiency was computed from an analysis of the trajectory of aerosol particles moving past falling ice crystal plates. Assuming that the flow around the aerosol particles does not affect the motion around the ice crystal (which is justified if the mass ratio of the particle to the drop is $\leqslant 10^{-3}$), the aerosol particle trajectory was determined from a solution to the equation

$$\frac{d\mathbf{v}}{dt} = m\mathbf{g} - \frac{6\pi\eta_a r}{(1 + \alpha \mathrm{N_{Kn}})}(\mathbf{v} - \mathbf{u}) + \mathbf{F}_{\mathrm{Th}} + \mathbf{F}_{\mathrm{Df}} \quad (1)$$

Eq. (1) applies to an aerosol particle of radius r, mass m and velocity $\mathbf{v}$, moving around an ice crystal of radius a_c, both falling in air of dynamic viscosity η_a, under the effect of gravity, hydrodynamic forces and phoretic forces. In Eq. (1) $\mathbf{g}^* = \mathbf{g}(\rho_p - \rho_a)/\rho_p$, $\mathbf{g}$ is the acceleration of gravity, ρ_p is the bulk density of the aerosol particle, ρ_a the density of air, $\mathrm{N_{Kn}} = \lambda_a/r$ is the Knudsen number, λ_a is the free path length of air molecules, $\mathbf{u}$ is the velocity field in air around the falling drop, $\alpha = 1.26 + 0.44 \times \exp \times (-1.10\ \mathrm{N_{Kn}}^{-1})$ (see Pruppacher and Klett, 1978), $\mathbf{F}_{\mathrm{Th}}$ is the thermophoretic force given by (see Pruppacher and Klett, 1978)

$$\mathbf{F}_{\mathrm{Th}} = -\frac{12\pi\eta_a r(k_a + 2.5k_p\mathrm{N_{Kn}})k_a\nabla T}{5(1 + 3\mathrm{N_{Kn}})(k_p + 2k_a + 5k_p\mathrm{N_{Kn}})p}, \quad (2)$$

and $\mathbf{F}_{\mathrm{Df}}$ is the diffusiophoretic force given by (see Pruppacher and Klett, 1978)

$$\mathbf{F}_{\mathrm{Df}} = -6\pi r\eta_a \frac{0.74D_{va}M_a\nabla\rho_v}{(1 + \alpha\mathrm{N_{Kn}})M_w\rho_a}, \quad (3)$$

where k_a and k_p are the thermal conductivities of air and aerosol particle, respectively, D_{va} is the diffusivity of water vapor in air, T absolute temperature, ρ_v water vapor density in air, and M_w and M_a are the molecular weights of water and air. Eqs. (2) and (3) were evaluated from a knowledge of the vapor density and temperature distribution around the falling ice crystal. These distributions were determined previously by Pitter *et al.* (1974) from a numerical evaluation of the steady-state convective diffusion equation applied to an ice crystal plate of radius a_c idealized by a thin oblate spheroid of ice of axis ratio $b/a_c = 0.05$ (b is the minor semi-axis and a_c the major semi-axis of the oblate spheroid). The velocity fields $\mathbf{u}$ around falling ice crystals, necessary for both solving the convective diffusion equation and solving Eq. (1), were those determined by Pitter *et al.* (1973) (for $\mathrm{N_{Re}} = 2a_cV_\infty/\nu_a \leqslant 20$), and by us (for $\mathrm{N_{Re}} = 50$) from a numerical solution of the complete Navier-Stokes equation of motion for steady state, incompressible flow of various Reynolds numbers (V_∞ is the terminal velocity of the ice crystal and ν_a the kinetic viscosity of air).

From a knowledge of the particle trajectory around the crystal the collision efficiency

$$E = \frac{\pi y_c^2}{\pi(a_c + r)^2} \quad (4)$$

was deduced, where y_c is the largest horizontal offset the particle can have and still collide with the crystal (y_c being measured perpendicular to the drop's axis aligned along $\mathbf{g}$, and sufficiently far upstream from the drop). The collision kernel was computed from Eq. (4) using the relation

$$K = E\pi(a_c + r)^2(V_{\infty,a} - V_{\infty,r}). \quad (5)$$

Model I just described was formulated and evaluated by Martin *et al.* (1980). In the present effort the results obtained with this model were combined with a second model (henceforth called model II) which applies to particles of $r < 0.1$ μm. Obviously, model I does not apply to this size range since this model does not include the effects of Brownian motion. In order to determine the efficiency with which aerosol particles of $r < 0.1$ μm are captured by simple ice crystal plates we developed model II in analogy to that formulated by Wang *et al.* (1978) and Wang (1979) for drops.

The collision efficiency in the present model II is found from a determination of the flux of aerosol particles to the collector ice crystal which falls at terminal velocity in air. The total particle current density $\mathbf{j}_p$ to the crystal can be written as $\mathbf{j}_p = n\mathbf{v}_p = n\mathbf{v}_{\text{drift}} - D_p\nabla n$, where $\mathbf{v}_{\text{drift}} = B_p\mathbf{F}_{\text{ext}}$, n is the number concentration of aerosol particles, $\mathbf{v}_{\text{drift}}$ their drift velocity, D_p their diffusivity, $B_p = (1 + \alpha \mathrm{N}_{\text{Kn}})/6\pi r\eta_a$ is their mobility, and $\mathbf{F}_{\text{ext}}$ is the sum of the external forces acting on the particle.

For particles moving as a result of Brownian diffusion, thermophoresis, diffusiophoresis and gravitational forces toward an ice crystal *at rest*, one finds

$$\mathbf{j}_p = nB_p(m\mathbf{g}^* + \mathbf{F}_{\text{Th}} + \mathbf{F}_{\text{Df}}) - D_p\nabla n. \quad (6)$$

We shall assume steady-state, constant diffusivity and further assume that the aerosol particles are small so that the term $m\mathbf{g}^*$ may be neglected in comparison to $\mathbf{F}_{\text{Th}}$, $\mathbf{F}_{\text{Df}}$ and $D_p\nabla n$ (a numerical evaluation of these forces shows that for typical conditions, the contribution of $m\mathbf{g}^*$ to the collision kernel is by several orders of magnitude smaller than the contribution of the phoretic forces and Brownian diffusion). The condition of particle continuity $(\partial n/\partial t) + \nabla\cdot(n\mathbf{v}_p) = 0$ leads to $\nabla\cdot\mathbf{j} = 0$, from which for an *ice crystal at rest*

$$B_p(\mathbf{F}_{\text{Th}} + \mathbf{F}_{\text{Df}})\cdot\nabla n - D_p\nabla_n{}^2 = 0. \quad (7)$$

In order to arrive at Eq. (7) we assume that

$$\nabla\cdot[n(\mathbf{F}_{\text{Th}} + \mathbf{F}_{\text{Df}})] = (\mathbf{F}_{\text{Th}} + \mathbf{F}_{\text{Df}})\cdot\nabla n, \quad (8)$$

which in turn requires that

$$\nabla\cdot(\mathbf{F}_{\text{Th}} + \mathbf{F}_{\text{Df}}) = 0. \quad (9)$$

This is justified for a *stationary ice crystal* whose temperature and vapor density fields are described by the solution to the Laplace equations

$$\nabla^2 T = 0, \quad (10a)$$

$$\nabla^2\rho_v = 0. \quad (10b)$$

Since from Eqs. (2) and (3) $\mathbf{F}_{\text{Th}} \propto \nabla T$ and $\mathbf{F}_{\text{Df}} \propto \nabla\rho_v$, it follows that Eq. (9) fulfills Eqs. (10a) and (10b).

However, for an *ice crystal falling at terminal velocity* the temperature and vapor density distribution, and hence ∇T and $\nabla\rho_v$ cannot be determined from Eqs. (10) but must be determined from solutions to the convective diffusion equation

$$\mathbf{u}\cdot\nabla T = \kappa_a\nabla^2 T, \quad (11a)$$

$$\mathbf{u}\cdot\nabla\rho_v = D_{va}\nabla^2\rho_v, \quad (11b)$$

where $\mathbf{u}$ is the velocity field in air around the crystal and κ_a is the heat diffusivity in air. From this, in turn, the enhancement of the heat and vapor flux due to the presence of an air flow past the crystal can be found. This enhancement can be expressed in terms of an angular dependent ventilation coefficient $f_v(\theta)$, $f_h(\theta)$ and $f_p(\theta)$ for water vapor, heat and particle transport, respectively, (where θ is the angle measured from the forward stagnation point of the crystal), or in terms of an overall ventilation coefficient $\bar{f}_v$, $\bar{f}_h$ and $\bar{f}_p$ for vapor, heat and particle transport, respectively. Values for an overall ventilation coefficient for ice crystals have been derived by Pitter *et al.* (1974) and by Hall and Pruppacher (1976).

In the present problem we are considering the overall flux of particles to a falling crystal. We are therefore only interested in the overall, flow-field-enhanced flux of particles to the crystal. Thus, neglecting the hydrodynamic drag force on the aerosol particle (which is very small, indeed, due to the very small fall velocity of the particle) we may write Eq. (7) for a *falling ice crystal* as

$$B_p(\bar{f}_h\mathbf{F}_{\text{Th}} + \bar{f}_v\mathbf{F}_{\text{Df}})\cdot\nabla n - \bar{f}_p D_p\nabla^2 n = 0. \quad (12)$$

In order to arrive at Eq. (12) we assumed, instead of (9)

$$\nabla\cdot(\bar{f}_h\mathbf{F}_{\text{Th}} + \bar{f}_v\mathbf{F}_{\text{Df}}) = 0, \quad (13)$$

where $\bar{f}_h$ and $\bar{f}_v$ are mean quantities over the body, and only a function of N_{Re} and $\mathrm{N}_{\text{Sc},v} = \nu_a/D_{va}$ (where ν_a is the kinematic viscosity of air, and N_{Re} and $\mathrm{N}_{\text{Pr}} = \nu_a/\kappa_a$, respectively (see Pruppacher and Klett, 1978). Recalling again that $\mathbf{F}_{\text{Th}} \propto \nabla T$ and $\mathbf{F}_{\text{Df}} \propto \nabla\rho_v$, Eq. (13) fulfills Eqs. (10a) and (10b).

In order to solve Eq. (12) it is necessary to determine $\mathbf{F}_{\text{Th}}$ and $\mathbf{F}_{\text{Df}}$ for a *stationary ice crystal*. This requires knowledge of the temperature and vapor density fields around a *stationary ice crystal*, which can be found from a solution of Eqs. (10a) and (10b) for the case of an ice crystal plate whose shape is idealized by that of a thin oblate spheroid of axis ratio AR = 0.05. Transforming these equations into oblate spheroidal coordinates ξ, η (see Pitter *et al.*, 1973) and solving them subject to the conditions $T(\xi = \xi_0) = T_s$, $\rho(\xi = \xi_0) = \rho_s$ and $T(\xi = \xi_\infty) = T_\infty$, $\rho(\xi = \xi_\infty) = \rho_\infty$, one finds

$$\nabla T = (T_\infty - T_s)\,\mathrm{sech}\xi\left[\frac{\pi}{2} - \sin^{-1}(\mathrm{AR})\right]^{-1} \times [a_c\,\mathrm{sech}\xi_0(\sinh^2\xi + \cos^2\eta)^{1/2}]^{-1}\hat{e}_\xi, \quad (14)$$

$$\nabla\rho_v = (\rho_{v\infty} - \rho_{vs})\,\mathrm{sech}\xi\left[\frac{\pi}{2} - \sin^{-1}(\mathrm{AR})\right]^{-1} \times [a_c\,\mathrm{sech}\xi_0(\sinh^2\xi + \cos^2\eta)^{1/2}]^{-1}\hat{e}_\xi. \quad (15)$$

With these solutions the phoretic forces can now be expressed for a *stationary* ice crystal as

$$\mathbf{F}_{\mathrm{Th}} = -\frac{12\eta_a r(k_a + 2.5k_p\mathrm{N}_{\mathrm{Kn}})k_a(T_\infty - T_s)G}{5(1 + 3\mathrm{N}_{\mathrm{Kn}})(k_p + 2k_a + 5k_p\mathrm{N}_{\mathrm{Kn}})p}\hat{e}_\xi, \quad (16)$$

$$\mathbf{F}_{\mathrm{Df}} = -6\pi r\eta_a\frac{0.74D_{va}M_a(\rho_{v\infty} - \rho_{vs})G}{(1 + \alpha\mathrm{N}_{\mathrm{Kn}})M_w\rho_a}\hat{e}_\xi, \quad (17)$$

where

$$G = \mathrm{sech}\xi\left[\frac{\pi}{2} - \sin^{-1}(\mathrm{AR})\right]^{-1} \times[a_c\,\mathrm{sech}\xi_0(\sinh^2\xi + \cos^2\eta)^{1/2}]^{-1}, \quad (18)$$

with $\xi_0 = \tanh^{-1}(\mathrm{AR})$.

For a *moving ice crystal* we shall now define

$$\bar{f}_h\mathbf{F}_{\mathrm{Th}} = GC_{\mathrm{Th}}\hat{e}_\xi, \quad (19a)$$

$$\bar{f}_v\mathbf{F}_{\mathrm{Df}} = GC_{\mathrm{Df}}\hat{e}_\xi, \quad (19b)$$

where $\hat{e}_\xi$ is the unit vector in ξ-direction, and where

$$C_{\mathrm{Th}} = -\frac{12\pi\eta_a r(k_a + 2.5k_p\mathrm{N}_{\mathrm{Kn}})k_a(T_\infty - T_s)\bar{f}_h}{5(1 + 3\mathrm{N}_{\mathrm{Kn}})(k_p + 2k_a + 5k_p\mathrm{N}_{\mathrm{Kn}})p}, \quad (20)$$

$$C_{\mathrm{Df}} = -6\pi r\eta_a\frac{0.74D_{va}M_a(\rho_{v\infty} - \rho_{vs})\bar{f}_v}{(1 + \alpha\mathrm{N}_{\mathrm{Kn}})M_w\rho_a}. \quad (21)$$

We shall now write Eq. (12) in the form

$$B_p\mathbf{F}_{\mathrm{ext}}\cdot\nabla\eta - \bar{f}_pD_p\nabla^2\eta = 0, \quad (22)$$

where

$$\mathbf{F}_{\mathrm{ext}} = (\bar{f}_h\mathbf{F}_{\mathrm{Th}} + \bar{f}_v\mathbf{F}_{\mathrm{Df}}) = CG\hat{e}_\xi \quad (23)$$

with

$$C = -(C_{\mathrm{Th}} + C_{\mathrm{Df}}) \quad (24)$$

and considering Eq. (18).

Writing Eq. (22) in oblate spheroidal coordinates one finds for $\xi = \xi_\infty$, $n = n_\infty$ and for $\xi = \xi_0$, $n = 0$ and using Eqs. (20), (21), (23) and (24), the solution

$$n = n_\infty\frac{\exp\left\{[-\beta C\sin^{-1}\tanh\xi]\left[\frac{\pi}{2} - \sin^{-1}(\mathrm{AR})\right]^{-1}\right\} - \exp\left\{[-\beta C\sin^{-1}(\mathrm{AR})]\left[\frac{\pi}{2} - \sin^{-1}(\mathrm{AR})\right]^{-1}\right\}}{\exp\left\{\left[-\frac{\pi}{2}\beta C\right]\left[\frac{\pi}{2} - \sin^{-1}(\mathrm{AR})\right]^{-1}\right\} - \exp\left\{[-\beta C\sin^{-1}(\mathrm{AR})]\left[\frac{\pi}{2} - \sin^{-1}(\mathrm{AR})\right]^{-1}\right\}}, \quad (25)$$

where $\beta = B_p/D_p\bar{f}_p$. Differentiation leads to

$$\nabla n = -\frac{n_\infty\beta C\,\mathrm{sech}\xi\left[\frac{\pi}{2} - \sin^{-1}(\mathrm{AR})\right]^{-1}\exp[-\beta C\sin^{-1}(\tanh\xi)]\hat{e}_\xi}{a_c\,\mathrm{sech}\xi_0(\sinh^2\xi + \cos^2\eta)^{1/2}\left\{\exp\left[-\frac{\pi}{2}\beta C\right] - \exp[-\beta C\sin^{-1}(\mathrm{AR})]\right\}}. \quad (26)$$

The total flux of particles to the crystal is

$$J_p = \int_s D_p\bar{f}_p(\nabla n)_{\xi=\xi_0}\cdot ds. \quad (27)$$

From Eq. (27) we find for the collision kernel $K = J_p/n_\infty$

$$K = \frac{4\pi B_pCa_c\,\mathrm{sech}\xi_0}{\left[\frac{\pi}{2} - \sin^{-1}(\mathrm{AR})\right]}\left[\exp\left(\frac{B_pC}{D_p\bar{f}_p}\right) - 1\right] \quad (28)$$

with $\xi_0 = \tanh^{-1}(\mathrm{AR})$. Using Eq. (28) the collision efficiency can be determined from

$$E = \frac{K}{\pi(a_c + r)^2(V_{\infty a} - V_{\infty r})}. \quad (29)$$

It is reasonable to assume that adhesive forces insure that an aerosol particle remains at the surface of an ice crystal after it had collided with it. The assumption is particularly justified at temperatures between 0 and −10°C at which water molecules have an appreciable surface mobility and behave as if they were part of a "pseudo-liquid" layer (see Pruppacher and Klett, 1978). With this assumption the collision efficiency E calculated by the above given procedure is then identical with the collection efficiency, and the collision kernel K is identical with the collection kernel.

3. Evaluation procedure

Models I and II were evaluated for platelike ice crystals idealized by an oblate spheroid of ice with an axis ratio (AR) = b/a_c = 0.05. The aerosol particles considered had radii of $0.001 \leq r \leq 10$ μm. The ice crystal plates had radii (i.e., semi-major axes) of a_c = 50.6, 87.9, 112.8, 146.8, 213, 289, 404 and 639 μm, corresponds to Reynolds numbers N_{Re} $(=2a_cV_\infty/\nu_a)$ = 0.1, 0.5, 1, 2, 5, 10, 20 and 50, respectively, at 700 mb and −10°C. In addition to this particular pressure-temperature level, models I

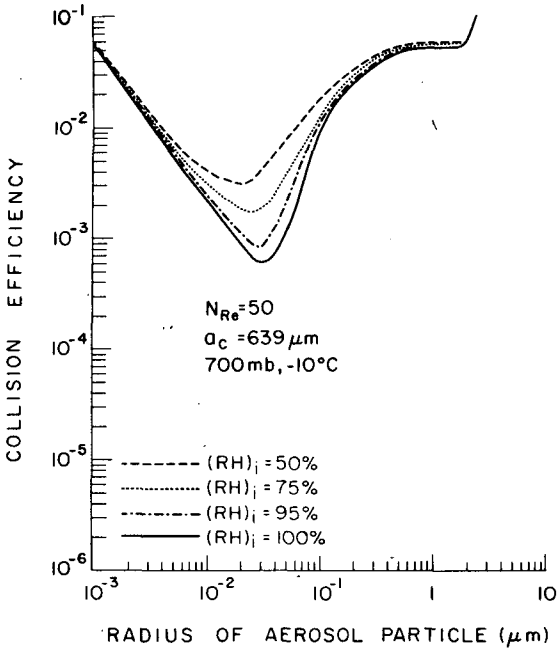

FIG. 1. Efficiency with which aerosol particles collide with simple planar ice crystals of radius a_c = 639 μm, and Reynolds number N_{Re} = 50 in air of 700 mb, −10°C and of relative humidity $(RH)_i$ (with respect to ice) of 50, 75, 95 and 100%; $\rho_p = 2 \times 10^{-3}$ kg m^{-3}.

and II were evaluated also for the levels 1000 mb, 0°C; 900 mb, −5°C; and 600 mb, −20°C. Due to the particular choice of corresponding pressure and temperature the Reynolds numbers corresponding to the above given crystal sizes were, with sufficient accuracy, the same at all levels considered. At each of these pressure levels we considered four relative humidities $(RH)_i$ (with respect to ice), viz., $(RH)_i$ = 100, 95, 75 and 50%. In a separate calculation we also considered the ambient air to be water saturated, i.e., $(RH)_w$ = 100%. The values chosen for $k_a(p,T)$, $\lambda_a(p,T)$, $D_{va}(p,T)$ and $\eta_a(T)$ were those recommended by Pruppacher and Klett (1978). The values for ρ_a were those given in the *Smithsonian Meteorological Tables*. The bulk densities of the particles considered were ρ_p = 1.0, 1.5, 1.75, 2.0 and 5 × 10^{-3} kg m^{-3}. In the present computations we also assumed that $\bar{f}_h \approx \bar{f}_v$, where $\bar{f}_v$ is the ventilation coefficient for water vapor transfer to the ice crystal, given by Hall and Pruppacher (1976). For evaluating $\bar{f}_p$ we assumed that its functional dependence on the Reynolds number and on the Schmidt number N_{Sc} is the same as that given by Hall and Pruppacher for $\bar{f}_v$, except that now instead of $N_{Sc,v} = \nu_a/D_{v,a}$ we used $N_{Sc,p} = \nu_a/D_{p,a}$, where $D_{p,a}$ is the diffusivity of aerosol particles in air. Values for $D_{p,a}$, and justifications for both of the above assumptions are given by Pruppacher and Klett (1978). The thermal conductivity of the aerosol particle material was assumed to be $k_p = 4.19 \times 10^{-1}$ J m^{-1} s^{-1} °C^{-1}. The variation of the collision efficiency with k_p was not studied since rough calculations showed that the collision efficiency is only weakly dependent on k_p.

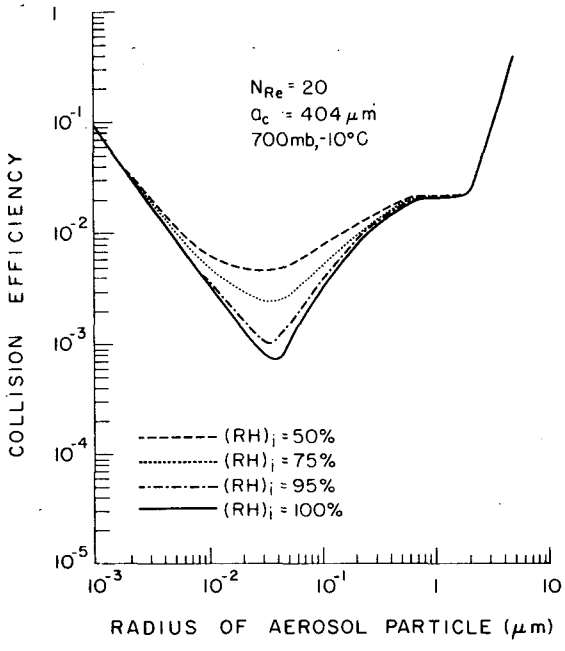

FIG. 2. As in Fig. 1 except for a_c = 404 μm and N_{Re} = 20.

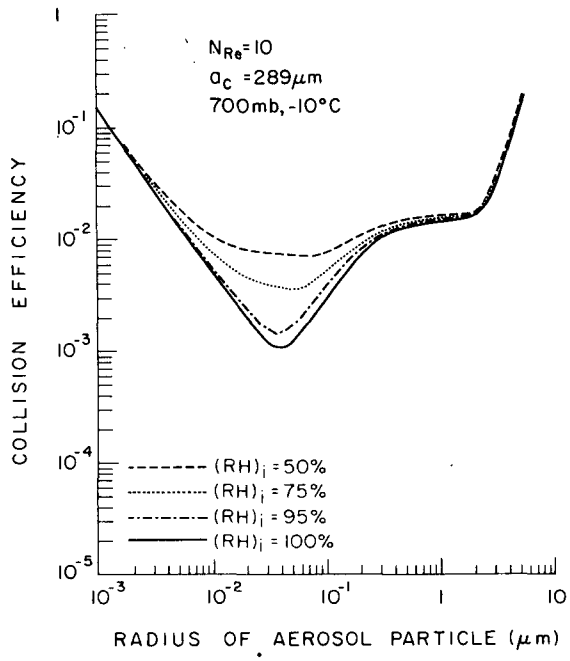

FIG. 3. As in Fig. 1 except for a_c = 289 μm and N_{Re} = 10.

4. Results and discussion

In Figs. 1–8 the major results of our study are summarized. These figures describe the efficiency with which aerosol particles of radii varying between

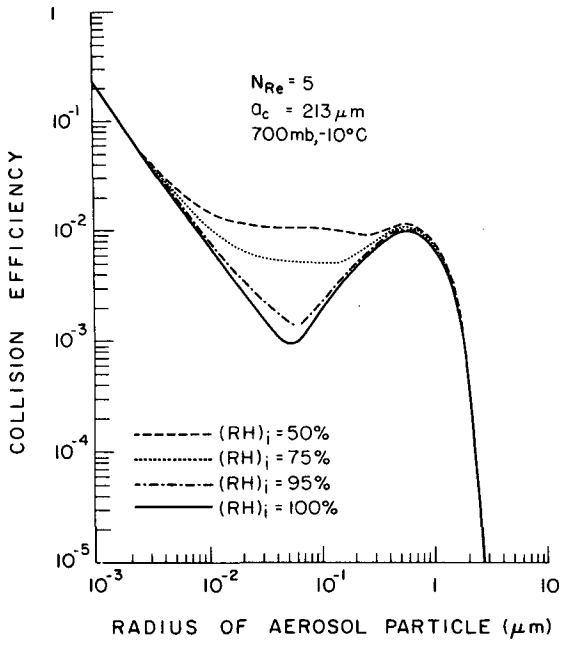

FIG. 4. As in Fig. 1 except for a_c = 213 μm and N_{Re} = 5.

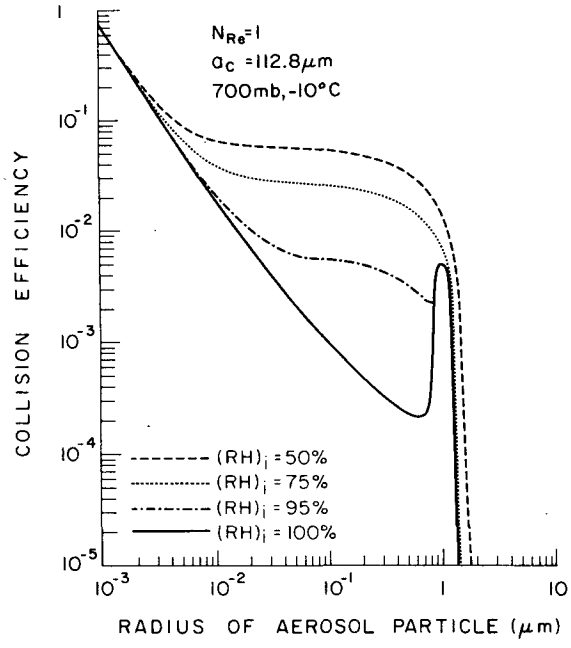

FIG. 6. As in Fig. 1 except for a_c = 112.8 μm and N_{Re} = 1.

0.001 and 10 μm are captured by simple plate-like ice crystals of various radii in air of various relative humidities and at −10°C at 700 mb. The results obtained for the other pressure-temperature levels specified above differed only insignificantly from those at −10°C and 700 mb and are therefore not shown here. We attribute this finding to our particular choice of pressure-temperature combination. Combinations of pressure and temperature other than those specified above may well change the present curves.

The most significant feature of the curves in Figs. 1–8 is the predominant minimum in the collision efficiency E for aerosol particles of radius between

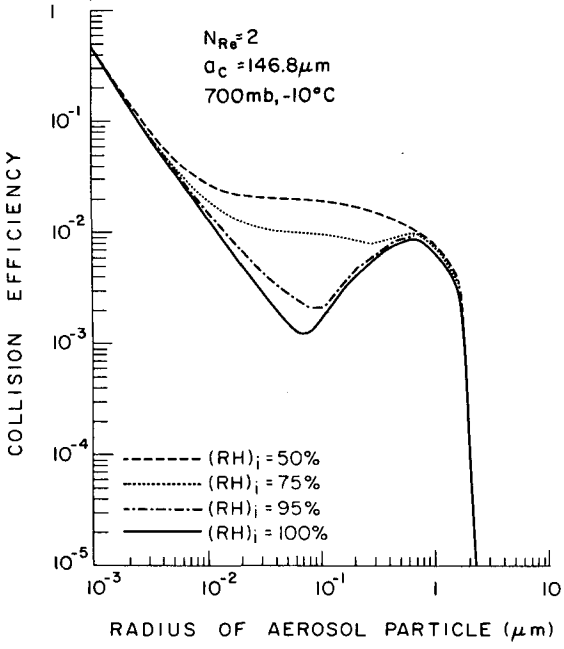

FIG. 5. As in Fig. 1 except for a_c = 146.8 μm and N_{Re} = 2.

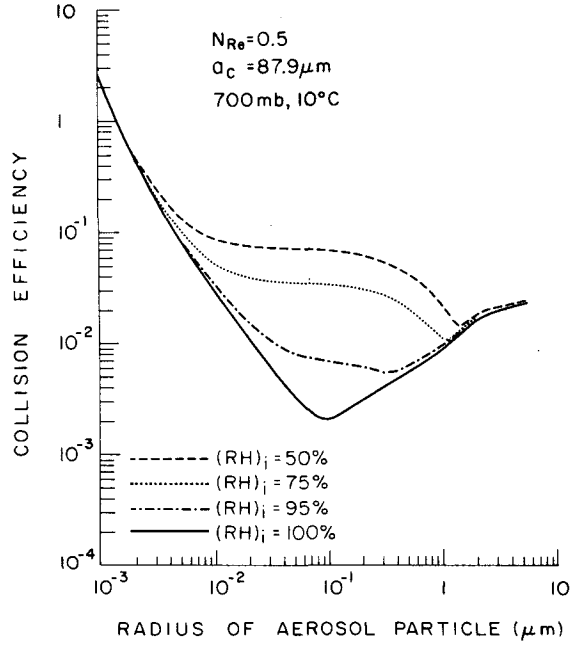

FIG. 7. As in Fig. 1 except for a_c = 87.9 μm and N_{Re} = 0.5.

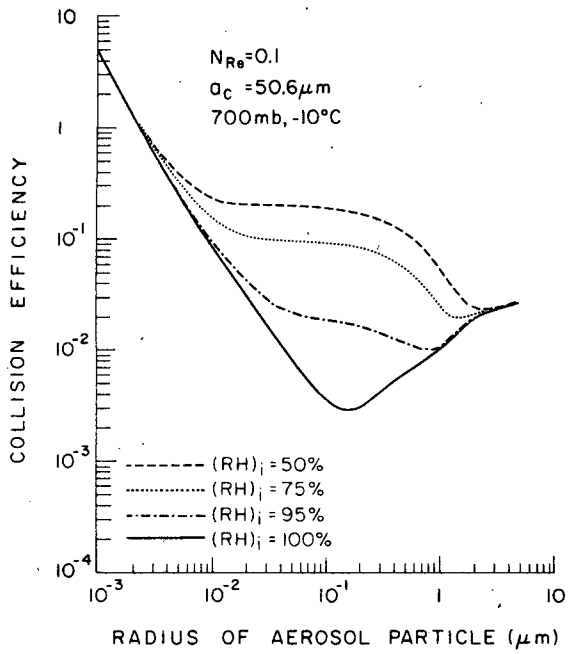

FIG. 8. As in Fig. 1 except for a_c = 50.6 μm and N_{Re} = 0.1.

r = 0.01 μm and r = 0.1 μm. Analogous to the particle scavenging behavior of water drops (see Wang *et al.*, 1978) this result is due to the fact that Brownian diffusion increasingly dominates scavenging if $r < 0.01$ μm while inertial impaction increasingly dominates scavenging if $r > 0.1$ μm. It is worth noting that this minimum (termed by Wang *et al.* as the "Greenfield gap") in particle collection efficiency is found within a particle size range which is about one order of magnitude smaller than the size range in which the minimum appears for scavenging by water drops. This implies that inertial capture extends its scavenging effect to a particle size which is considered smaller for ice crystal plates as scavengers than for water drops as scavengers. We shall show below that this is a result of the unusual properties of the ice crystal rim as a trap for the aerosol particles.

As in the case of particle scavenging by drops, particle scavenging by ice crystal plates is most strongly affected by phoretic forces in the Greenfield-Gap. This is quite evident from Figs. 1–8. On the other hand, the phoretic effects are quite small for aerosol particles of $r > 1$ μm and of $r < 0.01$ μm. Note also from Figs. 1–8 that the phoretic effects become stronger the smaller the ice crystal. Obviously, the smaller the ice crystal, the smaller the particle deflecting effect of the flow field beneath the crystal and therefore the stronger the phoretic effects. Thus, for sufficiently small ice crystals a change from 100 to 50% relative humidity (with respect to ice) causes an increase in the collision efficiency of up to two orders of magnitude.

Figs. 1–8 also show some very interesting behavior of the collision efficiency E if the aerosol particles have radii $r > 1$ μm. Thus, we note that for ice crystal plates of N_{Re} = 50, 20 and 10, E *increases* with r (see Figs. 1–3). For smaller ice crystal plates a dramatic change in behavior is noted. Thus, for crystals of N_{Re} = 5, 2 and 1, E *decreases* with increasing r (see Figs. 4–6). In fact, no particles are collected by ice crystals with these Reynolds numbers for $r > 2$ μm. Trajectory analysis shows that the reason for this behavior lies in the fact that at these relatively low Reynolds numbers the velocity with which an aerosol particle approaches an ice crystal has become small enough so that the strong horizontal hydrodynamic deflecting forces have sufficient time to move aerosol particles of $r > 2$ μm around the crystal. A second dramatic change in the collision behavior of ice crystal plates is found if ice crystals have $N_{Re} < 1$ (see Figs. 7 and 8). We note that at these very low Reynolds numbers ice crystal plates regain their capability of capturing aerosol particles of $r > 1$ μm. Analysis of the velocity field around the falling crystal shows that the reason for this behavior lies in a pronounced decrease of the horizontal, particle-deflecting velocity if $N_{Re} < 1$. In fact, the deflecting force for $N_{Re} < 1$ decreases to such a low value that despite the small approach velocity, the particle cannot escape colliding with the crystal.

Fig. 9 demonstrates that for the case of ice crystals situated in ambient air of $(RH)_i < 100\%$ the thermophoretic force $\mathbf{F}_{Th}$ on an aerosol particle dominates the diffusiophoretic force $\mathbf{F}_{Df}$ if $r \leq 2$ μm. Therefore if an ice crystal is evaporating the net phoretic force is directed toward the crystal aiding particle

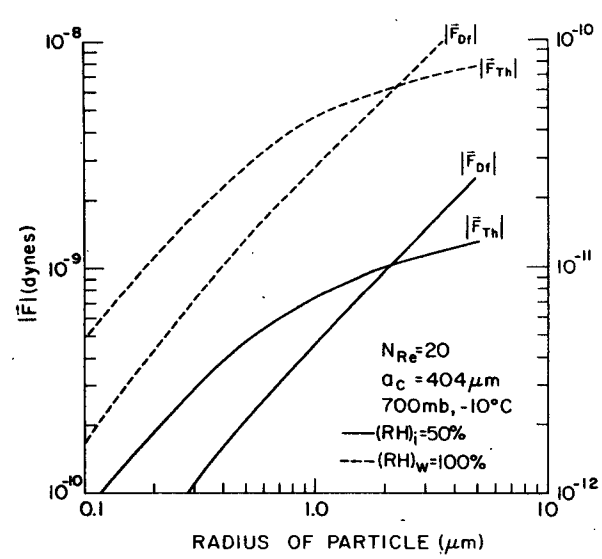

FIG. 9. Variation with particle size of the thermophoretic and diffusiophoretic force on aerosol particles moving around a simple planar ice crystal of 404 μm radius in air of $(RH)_i$ = 50%, and of $(RH)_w$ = 100%; $\rho_p = 2 \times 10^{-3}$ kg m^{-3}.

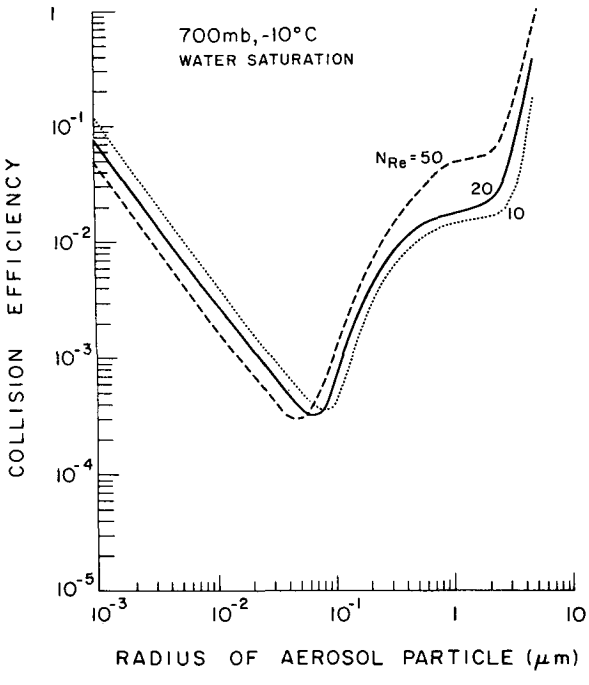

FIG. 10. Efficiency with which aerosol particles collide with simple planar ice crystals of radius a_c = 289 μm (N_{Re} = 10); a_c = 404 μm (N_{Re} = 20), and a_c = 639 μm (N_{Re} = 50), in water saturated air, $(RH)_w$ = 100%, of 700 mb, −10°C; $\rho_p = 2 \times 10^{-3}$ kg m^{-3}.

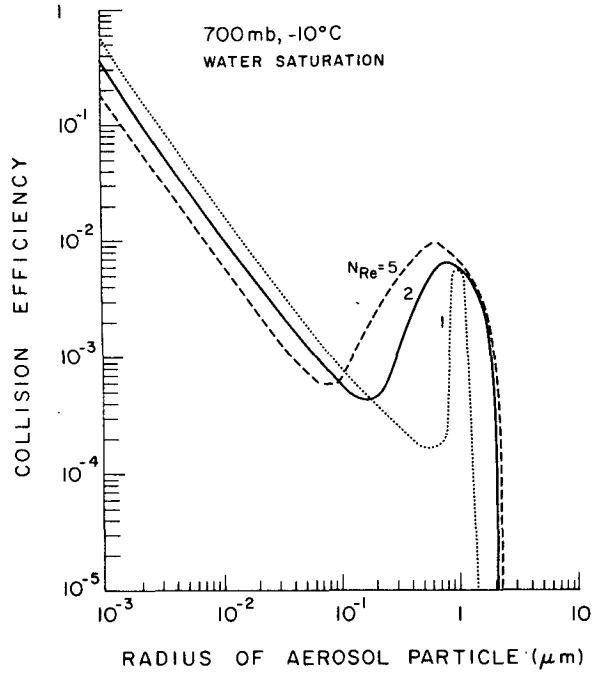

FIG. 11. As in Fig. 9 except for a_c = 213 μm (N_{Re} = 5), a_c = 146.8 μm (N_{Re} = 2), and a_c = 112 μm (N_{Re} = 1).

scavenging more the lower the relative humidity (with respect to ice saturation). For particles of $r > 2$ μm the trend reverses. However, for these large particles inertial capture completely dominates particle scavenging.

The situation changes dramatically if an ice crystal is situated in a mixed cloud consisting of ice crystals *and* supercooled water drops. In such a cloud the air is saturated with respect to water, i.e., $(RH)_w$ = 100%. Since for such a condition the ambient air is supersaturated with respect to ice, i.e., $(RH)_i$ > 100% an ice crystal will be growing by vapor deposition and therefore have a surface temperature warmer than the surroundings. The thermophoretic force and, since $|F_{Th}| > |F_{Df}|$ for $r \leq 2$ μm, the net phoretic force is therefore directed away from the crystal surface. The efficiency with which ice crystals collect aerosol particles in water saturated air is therefore expected to be considerably less than in ice saturated or ice subsaturated air. This is verified in Figs. 10–12. The reduction in efficiency is particularly pronounced for $5 \times 10^{-2} \leq r \leq 1$ μm.

5. Experimental verification

As mentioned in Section 1, it is unfortunate that only few experiments are available with which our theoretical data could be compared. Nevertheless, it will be shown below that the few data available still lend themselves to some qualitative support of our theory:

1) In Table 1 we have listed the ice crystal sizes studied and their corresponding terminal velocities

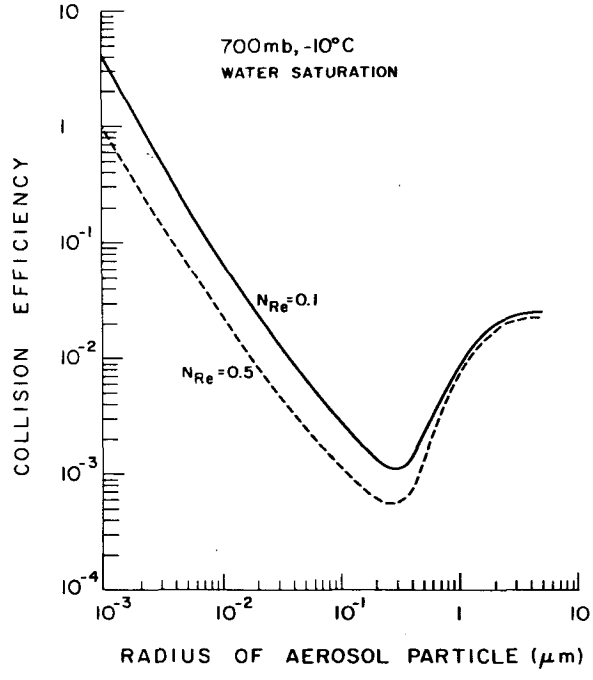

FIG. 12. As in Fig. 9 except for a_c = 87.9 μm (N_{Re} = 0.5) and a_c = 50.6 μm (N_{Re} = 0.1).

TABLE 1. Terminal fall speed of ice crystals at −15°C, 1000 mb.

N_{Re}	a_c (μm)	D_c (μm)	V_∞ [theory]* (cm s^{-1})	V_∞ [observation]** (cm s^{-1})
0.1	45	90	1.4	—
0.5	78	156	4.0	—
1	100	200	6.3	—
2	130	260	9.7	10
2.5	142	284	11.1	12.5
4	172	344	14.6	15
5	189	378	16.7	17
10	257	514	24.5	25
20	358	716	35.2	35
50	556	1112	56.7	57
100	802	1604	78.7	80

* $\rho_{ice} = 0.9$ g cm^{-3}; for oblate spheroid AR = 0.05.
** Simple hexagonal plates (Kajikawa, 1972).

V_∞ computed from values of the drag coefficient c_D via the formula (see Pruppacher and Klett, 1978)

$$V_\infty = \left[\frac{8ga_c^2(\mathrm{AR})(\rho_c - \rho_a)}{3c_D\rho_a}\right]^{1/2}. \tag{30}$$

Values for c_D have been obtained by Pitter *et al.* (1978) and by us from the streamfunction and vorticity fields around the ice crystals (see Pruppacher and Klett, 1978). The theoretically derived values for V_∞ for an oblate spheroidally shaped ice crystal plate of AR = 0.05 is compared in Table 1 with observed terminal velocities of simple ice crystal plates. Comparison of experiment and theory shows satisfactory agreement.

2) The collision efficiency curves (Figs. 1–3, Fig. 10) exhibit a pronounced "shoulder" at $0.5 \leq r \leq 5$ μm. This feature implies that in this size range an increase in size of the aerosol particle is accompanied by only a very small increase in efficiency with which it is captured by an ice crystal. Analysis of the trajectories of the aerosol particles involved in this effect shows that in this size range two compensating effects are at work. Thus, the larger the aerosol particle the easier it penetrates across streamlines to the surface of the ice crystal; thus it is expected to be collected with a larger efficiency than the smaller particle. However, with increasing proximity to the crystal surface the horizontal component of the velocity field rises rapidly so that the horizontal deflecting force on the particle compensates for its capability to approach closer to the crystal. The net effect of this behavior is that the collision efficiency of the large particle differs little from that of the smaller particle. A reanalysis of the experimental results obtained by Sood and Jackson[1] for planar snow crystal of $a_c = 1.5$ mm suggests that the shoulder theoretically predicted in the collision efficiency curve (Fig. 13) is also found in the experimentally derived curve. Unfortunately, the size of the collector ice crystal experimentally studied is considerably larger than the size of the collector crystals considered in the present study. This difference in size may account for the difference in the position of the Greenfield gap.

3) In Fig. 14 our theoretically predicted collision efficiencies are combined with those experimentally observed by Knutson *et al.* (1976). We notice that theory and experiment complement each other well. We notice further that, analogous to water drops, for an aerosol particle of a given size, the collision efficiency E undergoes a maximum at a certain crystal size $a_{c,\max}$. If $a_c > a_{c,\max}$($a_{c,\max} \approx 1000$ μm for $r \approx 0.7$ μm) the experiment shows that E decreases with increasing a_c, in analogy to the decrease with collector size found for drops by Wang *et al.* (1978). However, in contrast to drops, where the decrease in E with increase in *drop size* was explained in terms of eddy shedding from the rear of the drop allowing less and less aerosol particles to be captured in the rear as the shedding frequency increases, the decrease of E with increase in *ice crystal size* is a result of ice crystal oscillation which is the more pronounced the larger the crystal. Shedding of eddies from the rear of a hexagonal plate sets in if $N_{Re} \approx 50$ ($a_c \approx 1000$ μm). The larger the oscillation amplitude of the crystal the smaller the effective volume of air swept out by the crystal, and therefore the smaller the chance for particle capture. In contrast to drops, trajectory analysis shows that electrically uncharged ice crystals do not capture any aerosol particle on the rear side of a crystal unless the crystal oscillates or tumbles.

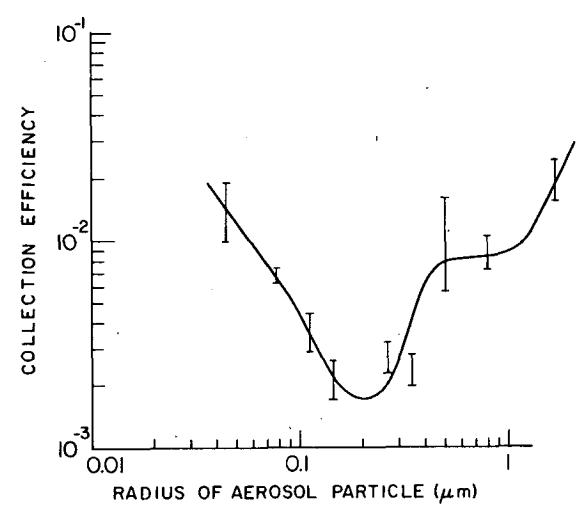

FIG. 13. Experimentally found variation of the efficiency with which aerosol particles are collected by planar ice crystals of $a_c = 1.5$ mm. Based on data of Sood and Jackson (1969).

[2] During their experiments the relative humidity of the air in the outdoor chamber was *not* recorded. However, the dates at which observations were made were noted. For these days we have obtained relative humidities using the observations of the Chicago Office of the National Weather Service.

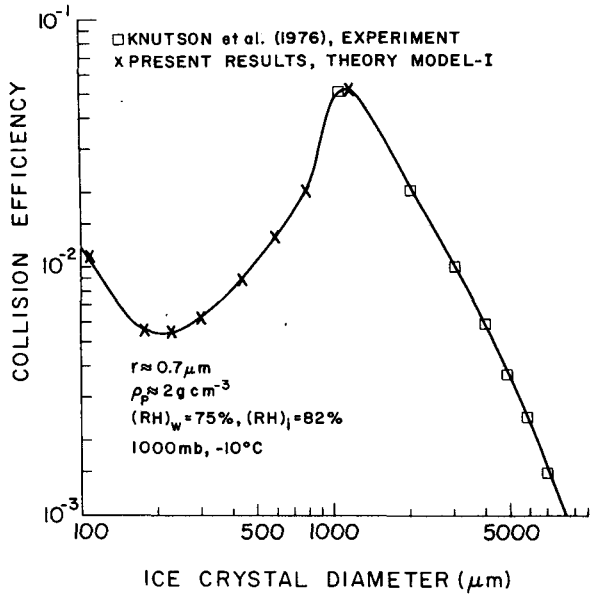

FIG. 14. Experimentally found variation of the efficiency with which aerosol particles of $r \approx 0.7$ μm are collected by planar ice crystals (based on data of Knutson *et al.*, 1967).

For ice crystals with $a_c < a_{c,\text{crit}}$ the present theory shows that the capture efficiency for aerosol particles of $r \approx 0.7$ μm decreases with decreasing a_c assuming a minimum value near $a_{c,\min} \approx 200$ μm. This behavior is expected on account of the fact that with decreasing a_c, i.e., decreasing N_{Re} of the collector, the inertial contributions to particle capture rapidly decreases. For $a_c < a_{c,\min}$ E reverses its trend and increases again with decreasing crystal size. This behavior is the result of the fact, that with decreasing N_{Re} of the crystal, the strength of the flow field around the crystal and the effect of this field to deflect the particle decreases with decreasing Reynolds number, i.e., decreasing size of the crystal, thus causing the phoretic forces to play an increasingly dominating role.

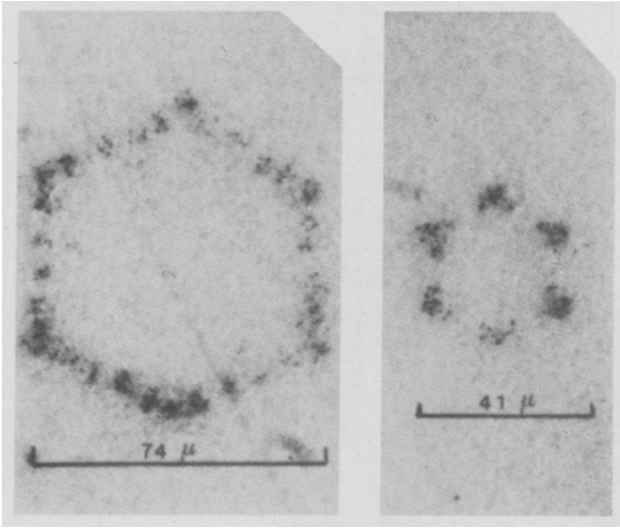

FIG. 15. Distribution of aerosol particles on the surface of planar ice crystals. Aerosol particles were captured by crystals while freely falling through an aerosol chamber filled with aerosol particles of $0.1 \leq r \leq 1.0$ μm. Note the preferred particle location of the particles at crystal edge. (Photographs taken by Prodi, 1976; reproduced by courtesy and permission of F. Prodi.)

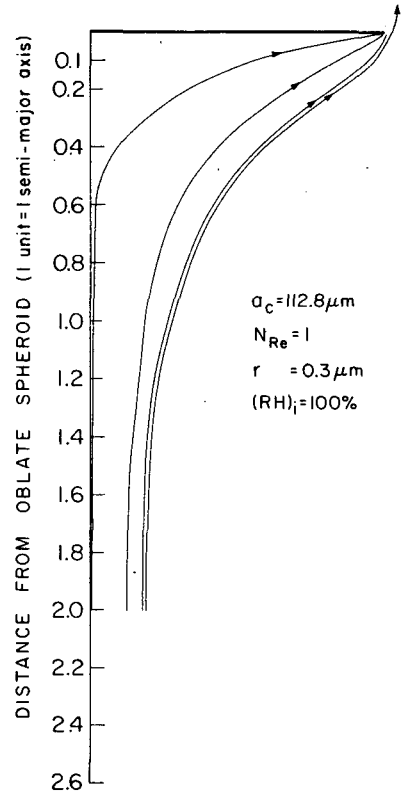

FIG. 16. Theoretically computed trajectory of an aerosol particle of $r = 0.3$ μm around a planar ice crystal of $N_{Re} = 1$ ($a_c = 112.8$ μm).

4) The distribution of aerosol particles of 0.1 μm $\leq r \leq 1$ μm captured on the surface of simple hexagonal ice plates has photographically been recorded by Prodi.[3] A typical distribution of aerosol particles on ice crystal plates is reproduced in Fig. 15. We note that most aerosol particles are captured by the ice crystal's rim. This result is in excellent agreement with our theoretical predictions summarized in Fig. 16. This figure shows various trajectories of aerosol particle of $r = 3$ μm moving around an ice crystal of $a_c = 112.8$ μm in ice saturated air. We note that the strong horizontal air flow beneath an ice crystal deflects all aerosol particles toward the rim of the crystal even if

[3] Prodi, F., 1976: Scavenging of aerosol particles by growing ice crystals. *Preprints Int. Conf. Cloud Physics*, Boulder, Amer. Meteor. Soc., 70–75.

a particle started off its trajectory very close to the crystal's fall axis.

Unfortunately, present experimental evidence is still far too small and too qualitative to verify quantitatively our theoretical predictions. However, the comparison possible as of now is encouraging.

Finally, we wish to emphasize that our present theoretical predictions do not include the effects of turbulence. It is expected that turbulence most likely will raise the collision efficiency in the Greenfield gap, particularly the efficiency of small collector crystals. Also, transient effects, such as those which occur when supercooled drops closely approach an ice crystal releasing water vapor toward the ice crystal in form of a directed vapor gush, were not considered by our present model.

Acknowledgments. The present study was supported by the Atmospheric Sciences Section, National Science Foundation, under Grant ATM 78-10817, by the Environmental Protection Agency under Grant R806257-02-1, and by Lawrence Livermore Laboratories under Grant PO 7683403. The authors would also like to express their sincere thanks to F. Prodi for providing them with the photographs reproduced in Fig. 15 of this article.

REFERENCES

Carnuth, W., 1967: Zur Abhaengigkeit des Aerosol Partikel Spektrum von meteorologischen Vorgaengen und Zustaende. *Arch. Meteor. Geophys. Bioklim.*, **A16**, 321–343.

Graedel, T. E., and J. P. Franey, 1975: Field measurements of submicron aerosol washout by snow. *Geophys. Res. Lett.*, **2**, 325–328.

Grover, S. N., H. R. Pruppacher and A. E. Hamielec, 1977: A numerical determination of the efficiency with which spherical aerosol particles collide with spherical water drops due to inertial impaction and phoretic and electric forces. *J. Atmos. Sci.*, **34**, 1655–1669.

Hall, W. D., and H. R. Pruppacher, 1976: The survival of ice particles falling from cirrus clouds in subsaturated air. *J. Atmos. Sci.*, **33**, 1995–2000.

Itagaki, K., and S. Koenuma, 1962: Altitude distribution of fallout contained in rain and snow. *J. Geophys. Res.*, **67**, 3927–3933.

Kajikawa, M., 1972: Measurement of falling velocity of individual snow crystals. *J. Meteor. Soc. Japan*, **50**, 577–584.

Knutson, E. O., S. K. Sood and J. D. Stockham, 1976: Aerosol collection by snow and ice crystals. *Atmos. Environ.*, **10**, 395–402.

Magono, C., T. Endoh and M. Itasaka, 1975: Observation of aerosol particles attached to falling snow crystals. *J. Fac. Sci. Hokkaido Univ.*, **4**, No. 4, 103–119.

——, ——, T. Hariyama and S. Kuboda, 1974: A measurement of scavenging effect of falling snow crystals on the aerosol concentration. *J. Meteor. Soc. Japan*, **52**, 407–416.

Martin, J. J., K. P. Wang and H. R. Pruppacher, 1980: On the efficiency with which aerosol particles of radius larger than 0.1 μm are collected by simple ice crystal plates. *Pure Appl. Geophys.* (in press).

Pitter, R. L., 1977: Scavenging efficiency of electrostatically charged thin ice plates and spherical aerosol particles. *J. Atmos. Sci.*, **34**, 1797–1800.

——, H. R. Pruppacher and A. E. Hamielec, 1973: A numerical study of viscous flow past thin oblate spheroid at low and intermediate Reynolds numbers. *J. Atmos. Sci.*, **30**, 125–134.

——, —— and ——, 1974: A numerical study of the effect of forced convection on mass transport from a thin oblate spheroid to air. *J. Atmos. Sci.*, **31**, 1058–1066.

Pruppacher, H. R., and J. D. Klett, 1978: *Microphysics of Clouds*. D. Reidell, 714 pp.

Radke, L. F., P. V. Hobbs and M. W. Eltgroth, 1980: Scavenging of aerosol particles by precipitation. *J. Appl. Meteor.*, **19**, 715–722.

Reiter, R., 1964: *Felder, Stroeme, Aerosole*. Verlag D. Steinkopff, 603 pp.

Reiter, R., and W. Carnuth, 1969: Washout Untersuchungen an Fallout Partikel in der unteren Troposphaere. *Arch. Meteor. Geophys. Bioklim.*, **A18**, 111–146.

Slinn, W. G. N., 1980: Precipitation scavenging. *Atmospheric Science and Power Productions 1979*, D. Randerson, Ed., U.S. Dept. of Energy, Tech. Info. Center, Oak Ridge, (see Chap. 2).

Starr, J. R., and B. J. Mason, 1966: The capture of airborne particles by water drops and simulated snow crystals. *Quart. J. Roy. Meteor. Soc.*, **92**, 490–499.

Wang, P. K., 1979: Particular solutions to the steady diffusion equation and their applications in aerosol scavenging problems. *Pap. Meteor. Res.*, **2**, 37–42.

——, and H. R. Pruppacher, 1977: An experimental determination of the efficiency with which aerosol particles are collected by water drops in subsaturated air. *J. Atmos. Sci.*, **34**, 1664–1669.

——, S. N. Grover and H. R. Pruppacher, 1978: On the effect of electric charge on the scavenging of aerosol particles by clouds and small rain drops. *J. Atmos. Sci.*, **35**, 1735–1743.